排灌机械工程学报
Journal of Drainage and Irrigation Machinery Engineering
2016 年 10 月 Oct. 2016 | 第 34 卷 第 10 期 Vol. 34 No. 10

Doi: 10.3969/j. issn.1674 - 8530.15.0241

Quantitative visualization of Taylor – Couette flow with helical protrusion using optical and ultrasound imaging method


KIM S. J.

KIM S. J.[1], TU X. C.[1], KIM H. B.[1,2]

(1. School of Mechanical and Aerospace Engineering, Gyeongsang National University, Jinju, Gyeongnam 660 - 701, Republic of Korea; 2. Research Center for Aircraft Parts Technology, Gyeongsang National University, Jinju, Gyeongnam 660 - 701, Republic of Korea)

Abstract: The simplified flow of drilling process in the soil hardening or oil rig site was experimentally investigated. Two flow models were used. One is the concentric cylinders with helical protrusion at the inner cylinder. The other is the concentric plain wall cylinders with axial flow. The radius ratio and aspect ratio of both models are the same with 0.65 and 48, respectively. The mud is the typical fluid seen in the soil hardening processes. We used the water and the mud for the working fluid. We used the optical PIV for the water flow measurement and echo PIV for the mud flow. In case of the water study, the dominant vortical structures appeared in both the protrusion and plain model with axial flow. In case of mud flow, the vortices shown in the water model disappeared and the push and pull-up motion by the protrusion is dominant. We believe this information can be useful to understand the flow physics of drilling process in the complex fluid flow.

Key words: Taylor – Couette flow; surface protrusion; echo PIV; mud flow

CLC Number: S277 **Document Code**: A **Article No**: 1674 - 8530(2016)10 - 0829 - 06

KIM S J, TU X C, KIM H B, et al. Quantitative visualization of Taylor – Couette flow with helical protrusion using optical and ultrasound imaging method[J]. Journal of drainage and irrigation machinery engineering(JDIME), 2016,34(10):829 - 834.

1 Introduction

Mud fluid flow is typical opaque flow which can be seen in offshore plants, oil rigs and soil hardening sites[1]. The physical nature of mud fluid is quite complex. It is non-Newtonian and opaque fluid as the mixture of heterogeneous materials. The properties of mud fluid have been studied in the rheology. For example, XU et al.[2] studied the rheological properties of steady and oscillatory mud flow at Lianyun Harbor in China.

The studies of mud flow are limited to some modeling, quantitative visualizations[3-4]. MRI and X-ray technique were applied to measure the quantitative velocity of the mud or sand flow[5]. It is still a challenging to get the velocity information from the mud flow.

One of the popular mud flow problem in the oil rig or soil hardening process is the rotating flow[6]. This is a kind of drilling process. These drilling processes can be simulated with Taylor – Couette flow with axial flow motion. Taylor – Couette flow is a kind of shear driven flow that occurred in the annular gap between two concentric cylinders. The transition of flow regime begins as the difference of rotating speeds between the inner and outer cylinder increases[7]. Previous studies showed the winded vortices in the annular gap of Taylor – Couette flow with the axial flow. The fluid transport between vortices for wavy vortex flow became

Received date: 2015 - 11 - 10; **Publish time on line**: 2016 - 10 - 08
Online Publishing: http://www.cnki.net/kcms/detail/32.1814.TH.20161008.1552.002.html
Author information: KIM S. J. (1989—), male, M. S. (udueve@gnu.ac.kr), researching in flow measurements.
TU X. C. (1984—), male, Ph. D. (tu0610@gnu.ac.kr), researching in heat exchanger, experimental method.
KIM H. B. (1971—), male, Ph. D., professor(kimhb@gnu.ac.kr), researching in flow measurement and control.

more evident too[8-9].

The axial flow generated by the surface protrusion of inner cylinder transports the cut material and let the drill move inward in the drilling process. Most of drilling process studies have been focused on the design of the drill rod itself such as thermal response, electric power demanded, and reliability. The flow transport of the mud or soil in the drilling process were less considered[10].

In this study, we experimentally investigated the drilling process using the simplified models. One is Taylor – Couette model with helical surface protrusion. The other is the plain Taylor – Couette model with axial flow. We also investigated the feasibility of mud flow measurement by using ultrasound imaging method. First, we measured the flow field and compared the difference between the protrusion and axial flow model using water as a working fluid. After that, we measured the mud flow in the protrusion model using echo PIV. Echo PIV is the combination of ultrasound B-mode imaging technique with PIV method and it is developed to measure the blood flow[11].

We believe this study helps the physical understanding of drilling process and presents the advanced experimental tool to study complex fluid flow.

2 Experimental apparatus and method

The geometries of the experimental models used in this study are shown in Fig. 1. The surface protrusion model and plain Taylor – Couette model with axial flow were made to simulate the drilling process. Fig. 1a shows the geometries of the cylinders for plain model. The radius of the inner cylinder (r_i) and the inner radius of the outer cylinder (r_o) were 13 mm and 20 mm, respectively. The annular gap (d) between the cylinders was 7 mm and the length of the cylinders (L) was 336 mm. We chose an aspect ratio (L/d) of 48, and the radius ratio (r_i/r_o) was 0.65 following the studies of COLE[12] and WERELEY[8]. Fig. 1b shows the configuration of surface protrusion model for simulating drill rod. A square protrusion with a cross section size of 5 mm × 5 mm was helically wrapped around the inner cylinder. The total radius, r_d, of this modified inner cylinder was 18 mm. The pitch (p) was 24.8 mm shown in Fig. 1c. These geometries were based on the previous study[10].

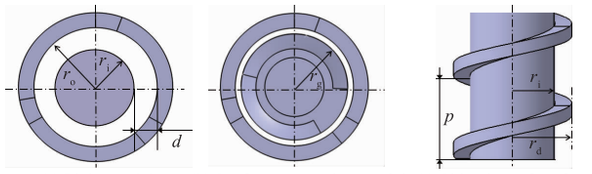

(a) Plain model (b) Surface protrusion model (c) Side view of surface protrusion model

Fig. 1 Geometries of experimental models

The experimental apparatus to optically measure the velocity fields is shown schematically in Fig. 2a and Fig. 2b and to measure the velocity fields using ultrasound method in Fig. 2c. We captured the synchronized image pairs at a fixed location to get the phase locked result due to the periodical appearance of protrusion in the image of surface protrusion model. The phase-averaged velocity filed was calculated from 100 pairs of images. We applied the conventional cross-correlation PIV method and the interrogation window size was 32 × 32 pixels with 50% overlapping.

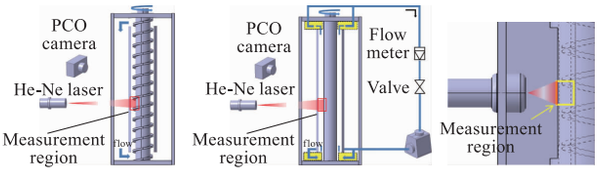

(a) Surface protrusion model (b) Plain-axial model (c) Ultrasound measurement

Fig. 2 Schematic diagram of experimental apparatus

The B-mode images were generated by a commercial ultrasound apparatus (Capistrano Lab Inc., USA) for mud flow measurement. The strength of echo signal from the scatters determines the bright intensity of image in B-mode. Time of flight is used to determine the location of the scatters. Sweeping (scanning) the beam builds up a two-dimensional echo image.

We used the probe which has 12.5 MHz center frequency. The depth of field is 18 mm. The ultrasound beam contains 64 vectors. The display angle of the transducer is 20°. We applied conventional cross-correlation based PIV method with window offsetting and the final interrogation window of 8 × 24 pixels.

The frame rate of ultrasound images is 60 fps. The

inner cylinder was driven by a micro stepper motor having a resolution of 400 000 steps per revolution. This micro stepper motor was controlled through a computer, which allowed for the precise control of angular speed and the acceleration to the preset velocity. The working fluid filling the annular gaps between the sets of concentric cylinders also filled the space between the outer cylinders and the boxes for the optical PIV measurement.

The rotating Reynolds number was defined as follows:

$$Re = r_i d\Omega/\nu, \qquad (1)$$

where d is the gap width, Ω is the angular velocity of the inner cylinder and ν is the kinematic viscosity of the working fluid.

The mud fluid properties were measured using the Rheometer (MCR 301). Fig. 3 shows the viscosity variance of wet mud with additional water addition, where r' is shear rate. Wet mud has about 0.5 mass fraction of dried mud/water ratios. We chose two mass fractions of 0.36 and 0.50 for this study.

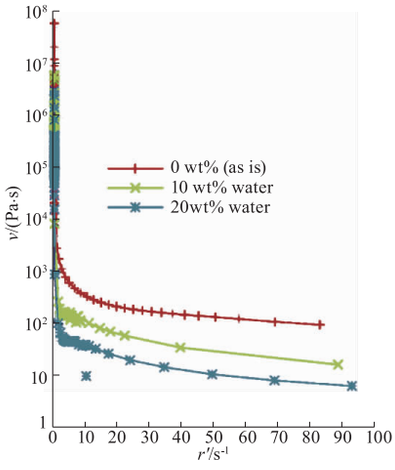

Fig. 3 Viscosity variance of wet mud with different water mass fractions according to shear rate

We found that when the mass fraction is above 0.66, most of the ultrasound signal severely attenuates and cannot penetrate into the mud flow. The accumulation of mud in front of the protrusion also becomes severe and it hinders the flow measurement from the preliminary test.

The axial flow rate (Q) for plain Taylor – Couette model was calculated based on the equation for the extruders[13]. Because our model has a wider gap ($\delta = r_o - r_d$) between the outer wall and the edge of protrusion compared with the extruder model, we believe this causes a little difference with the real axial flow rate generated by the surface protrusion.

The calculated flow rate Q is 5.05, 10.5, 19.1 and 26.0 cm^3/s for each Re number 50, 120, 220 and 300, respectively. In the plain-axial model, axial flow was driven and controlled by the centrifugal pump and flow meter.

3 Results and analysis

First, we measured the plain Taylor – Couette flow without the axial flow using optical PIV. This is the validation of our experimental method and models by comparing the results from the previous studies. Fig. 4 shows the averaged velocity fields of the radial-axial plane in the gap region. The axial position, $Z^* = z/d$, and the radial position, $R^* = (r - r_i)/d$, are normalized by the annular gap width. The contours represent the vorticity calculated from radial and axial velocities. When the Reynolds number was 50, there was no vortex in the annular gap. It is circular Couette flow regime. As the rotating Reynolds number increased to 120, the vortex pairs appeared in the annular gap. The axial size of the vortex was similar to the annular gap width of 1.1d. When the rotation speed of inner cylinder increased further, the vorticity of vortex pair became stronger. This is the same flow regime change of previous study[14] and confirms the validity of the experiments.

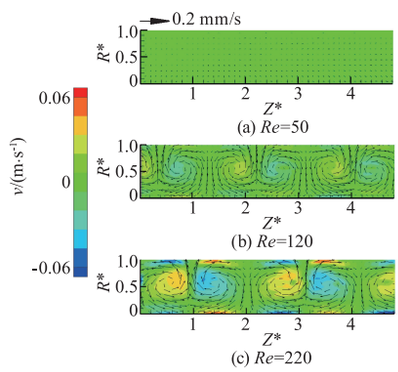

Fig. 4 Average velocity field of plain model

3.1 Plain Taylor – Couette model with axial flow

Fig. 5 shows the instantaneous velocity field of

plain Taylor – Couette model with axial flow for different Reynolds numbers. In the experiments, the axial flow moves in an opposite direction of gravity. It is the left direction in Fig. 5. When the Reynolds number was 50, there were no vortices in the flow field, the axial flow was dominant. With the increasing of the axial flow rate and rotating Reynolds number, the outward radial velocity appears periodically and becomes stronger. The counterclockwise rotating vortex flow appeared in the annular gap as the Reynolds number increases to 220. This is due to the strong negative axial velocity and positive radial velocity components. Owing to the winding effect of the axial flow, the helical vortex wraps around the inner cylinder. The counter-rotating vortices pair appears in the gap region when the Reynolds number is above 300.

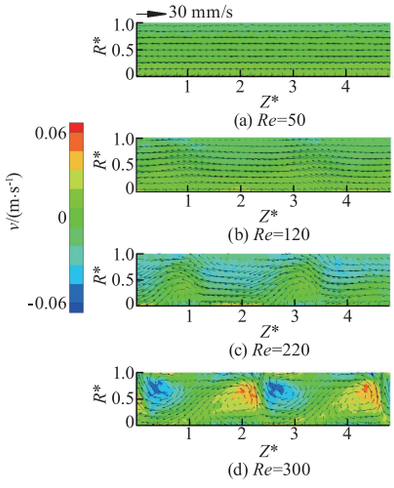

Fig. 5 Instantaneous velocity field of Taylor – Couette flow with axial flow model

The vortex pair does not have the symmetry like the plain Taylor – Couette flow. The vortices pair has elongated along the axial redirection. And the center line crossing the vortex cores rotates in the counterclockwise direction. From the results, the axial flow suppressed the occurrence of Taylor vortices and helps the asymmetric development of vortices pair compared with the plain Taylor – Couette flow.

3.2 Surface protrusion model

Fig. 6 shows the phase-averaged velocity field of the surface protrusion model. The drill rod rotates in the clockwise direction along the z-axis which looks like the upward movement and it is the left direction in Fig. 6. The shown velocity is not the absolute one, but the relative velocity which considers the surface protrusion is fixed. The existence of large counterclockwise rotating flows between the protrusions is clearly seen. The speed of upward flow at the wall of inner cylinder ($R^* = 0$) is faster than that of the downward flow at the wall of outer cylinder ($R^* = 1$). As the rotating Reynolds number increases, the relative velocities in the pitch region increase and small counterclockwise vortex in front of the protrusion appears.

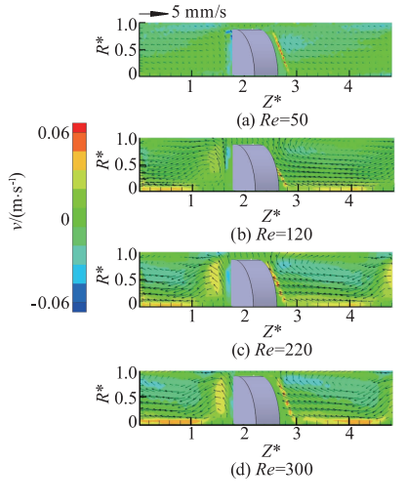

Fig. 6 Phase-averaged relative velocity fields of surface protrusion model

The relative velocities does not increase and got the asymptotic values as the rotating Reynolds number is above 220. In addition, the positive radial velocities exist around the leading and trailing edge of the protrusion. The flow structure of surface protrusion model is qualitatively similar to the flow field of plain Taylor – Couette model with axial flow at the intermediate Reynolds number case ($Re = 220$). The clockwise rotating vortex flow is dominant at the pitch region and the smaller counterclockwise rotating vortex appears in front of the protrusion. The fast upward flow in the wall of inner cylinder and the slow downward flow in the wall of outer cylinder also appear. Although the protrusion model shows a qualitatively similar flow structure with axial flow model, the counterclockwise rotating vortex is larger and the clockwise rotating vortex is smaller than that of plain Taylor – Couette model with axial flow.

3.3 Echo PIV experiment

The mud as a typical working fluid at drilling

processes in the soil hardening or oil rig sites is non-Newtonian and the complex fluids.

We performed echo PIV experiment to measure this complex fluid flow. We firstly applied it to the protrusion model using the water as a working fluid for validating the method.

The rotating Reynolds number is 120 in echo PIV measurement. Because the dynamic range of echo PIV is determined from the frame rate and the physical properties of ultrasound, we cannot measure the velocity field when the rotating Reynolds number is above 120. Fig. 7 is the comparison of average velocity filed of optical and echo PIV. The vector plot shows qualitatively the similar results between optical and echo PIV. Both of them extract the larger counterclockwise rotating vortex in the pitch region and smaller clockwise rotating vortex in front of the protrusion. Fig. 8 is the line data comparison of $Z^* = 1.2$ near the upper side of protrusion.

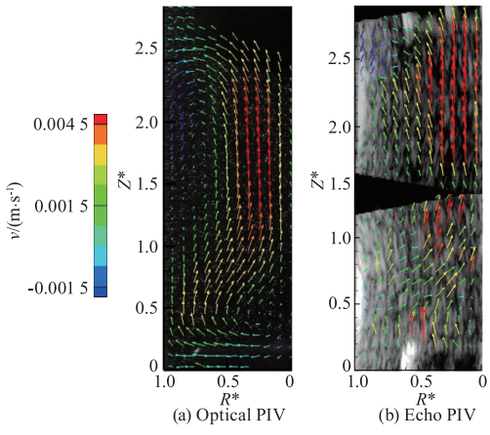

Fig. 7 Comparison of velocity field of surface protrusion model at Reynolds number of 120

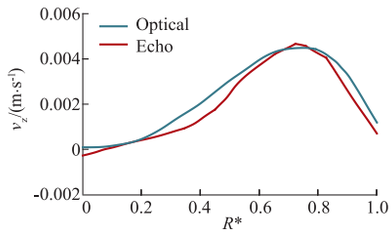

Fig. 8 Optical and echo PIV velocity comparison between optical and echo PIV at $Z^* = 1.2$ location

The results show the echo PIV can capture not only the qualitative flow structure but also the quantitative velocity information.

3.4 Mud flow measurement

The velocity of mud gap flow in the surface protrusion model was measured by using echo PIV. Fig. 9 shows the velocity field of pitch region for different mass fractions w. Regardless of the mass fraction, both cases show the clear difference compared with the results of the water experiments shown in Fig. 7. The magnitude of the relative velocity in the pitch region is smaller than that of water models. In addition, there are no large counterclockwise and small clockwise rotating vortices in the pitch region except the small vortex in the mid of pitch region. The strong outward radial velocity at the front and behind the protrusion of the model does not exist either. The push in front of the protrusion and the pull-up flow behind the protrusion is dominant in this mud fluid model. This result means that the mud fluid flow moves like the solid material in the near vicinity of the protrusion. Another difference compared with water model is that, there is the downward flow in the gap area between the outer cylinder and the edge of the protrusion. This leakage flow goes upward by pulling up the protrusion and generates the clockwise vortex flow.

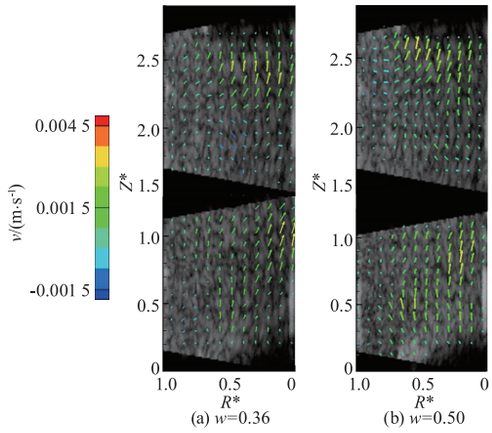

Fig. 9 Ultrasound velocity results at top and bottom of protrusion

4 Conclusions

In this study, we experimentally investigated the effect of surface protrusion of inner cylinder in the Taylor – Couette flow. When the working fluid is water, we found the protrusion generates the vortices pair which wrapped the pitch area of the inner cylinder.

This flow structure is similar to the plain Taylor – Couette model with axial flow in the intermediate Reynolds number. In case of the mud fluid as a working fluid, the flow structure changes drastically.

There is no dominant vortical structure in the pitch area. And the mud flow appears like the solid material in the vicinity of the protrusion and the leakage flow is clear at the gap between the protrusion and outer cylinder wall. We believe this information of flow fields helps the understanding of flow physics in the drilling process

Acknowledgements

The work was supported by Basic Science Research Program (2013 – 008918) through the National Research Foundation (NRF) and the Gyeongsang National University Fund for Professors on Sabbatical Leave, 2015.

References

[1] CHAKRABARTI S K. Handbook of offshore engineering [M]. Amsterdam: Elsevier, 2006.

[2] XU J Y, ZHANG J, HUHE A. Rheological investigation of natural mudflow at Lian-yun Harbor in China[C]// Proceedings of 8th International Conference on Multiphase Flow. Jeju: ICMF, 2013: 1 – 10.

[3] BECU L, GRONDIN P, COLIN A, et al. How does a concentrated emulsion flow?: Yielding, local rheology, and wall slip[J]. Colloids & surfaces A: physicochemical & engineering aspects, 2005, 263(1/2/3): 146 – 152.

[4] COUSSOT P. Mudflow rheology and dynamics [M]. Rotterdam: Balkema, 1997.

[5] PHAM V B, BRISSET P. Non intrusive devices applied to sedimentation and consolidation[C]//Proceedings of ASME – JSME – KSME 2011 Joint Fluids Engineering Conference. New York: ASME, 2011: 2741 – 2747.

[6] GROWCOCK F B, BELKIN A, FOSDICK M, et al. Recent advances in aphron drilling fluids[M]. London: Society of Petroleum Engineers, 2006.

[7] TAYLOR G I. Stability of a viscous liquid contained between two rotating cylinders[J]. Philosophical transaction of the royal society of London, 1923, 223: 289 – 343.

[8] WERELY S T, LUEPTOW R M. Velocity field for Taylor – Couette flow with an axial flow[J]. Physics of fluids, 1999, 11(12): 3637 – 3649.

[9] HWANG J Y, YANG K S. Numerical study of Taylor – Couette flow with an axial flow[J]. Computers & fluids, 2004, 33: 97 – 118.

[10] FINZI A E, LAVAGNA M, ROCCHITELLI G. A drill-soil system modelization for future Mars exploration[J]. Planetary and space science, 2004, 52: 83 – 89.

[11] KIM H B, HERTZBERG J R, SHANDAS R. Development and validation of echo PIV[J]. Experiment in fluids, 2004, 36: 455 – 462.

[12] COLE J A. Taylor-vortex instability and annulus-length effects [J]. J fluid mechanics, 1976, 75: 1 – 15.

[13] MIDDLEMAN S. Fundamentals of polymer processing [M]. New York: McGraw – Hill, 1977.

[14] LEE S H, CHUNG H T, PARK C W, et al, Experimental investigation of slit wall effects on Taylor – Couette flow[J]. Fluid Dyn Res, 2009, 41: 045502.

(特约编辑 赵凤朝 责任编辑 盛杰)